J Solid State Electrochem (2004) 8: 633–637
DOI 10.1007/s10008-004-0503-3

ORIGINAL PAPER

E. Gourba · P. Briois · A. Ringuedé · M. Cassir
A. Billard

Electrical properties of gadolinia-doped ceria thin films deposited by sputtering in view of SOFC application

Received: 11 April 2003 / Accepted: 29 September 2003 / Published online: 26 May 2004

Abstract Gadolinia-doped ceria (GDC) remains, up to now, the most promising candidate for replacing yttria-stabilised zirconia (YSZ) as electrolyte for solid oxide fuel cells (SOFC) operating at intermediate temperature. Literature data point out that GDC could be used as electrolyte, anode material, or interlayers for avoiding the chemical interactions occurring at the interfaces. In the present work, GDC thin layers were produced by d.c. reactive magnetron sputtering and deposited over a thickness domain between 450 nm and 5.5 μm. According to our knowledge, the deposition of GDC sputtered layers has never been reported. The physico-chemical features of these thin films have been characterised by X-ray diffraction (XRD) and scanning electron microscopy (SEM). Impedance measurements have been carried out in order to determine the electrical properties of electrolyte thin films and in particular their ionic conductivity.

Keywords Solid oxide fuel cell · Gadolinia-doped ceria · Thin layer · Sputtering · Impedance spectroscopy

Introduction

One of the solutions in order to reduce the SOFC operating temperature is the replacement of the state-of-the-art electrolyte, yttria-stabilised zirconia (YSZ). Nevertheless, this is not an easy problem because most of the materials with higher ionic conductivity than YSZ are also electronic conductors, which may induce potential losses and short-circuiting.

Ceria-based oxides are probably the most interesting candidates for a new SOFC generation as electrolytes and/or as catalysts in the anode side, most particularly for methane oxidation [1, 2, 3]. Among the compounds of this family, gadolinia-doped ceria (GDC) seems to be the most suitable, but it can also be an electronic conductor due to the reduction of Ce^{4+} at low oxygen partial pressures [4]. This redox reaction can be avoided either by adding a co-dopant to stabilise its structure [5, 6] or by reducing its thickness [7]. In the last case, an ultrathin layer of YSZ could act as an electronic barrier [8, 9]. In fact, combining the use of GDC with thin layer technology, including YSZ, can be a very efficient way to lower significantly the electrolyte resistance. Interesting results have been obtained with bi- or multi-layers of YSZ, YSB (yttria-stabilised Bi_2O_3) and YDC (yttria-doped CeO_2) [10].

In the recent literature, different deposition techniques have been used to produce thin layers of the SOFC electrolyte, mainly YSZ but also YSB and YDC, by magnetron sputtering [10, 11, 12, 13], vacuum plasma spray [14], polymeric spin coating [15] and screen printing [16]. In a previous paper, we have shown the interest of using RF magnetron sputtering of oxide targets and atomic layer deposition (ALD) to produce homogeneous GDC layers of 1 to 5 μm on lanthanum-doped manganite (LSM) [17]. As far as we know, no other works have been dedicated to the elaboration of dense GDC thin layers with thickness less than 5 μm by sputtering. Moreover, very few systematic works on the electrical properties of GDC thin layers are available in the literature. Recently, electrochemical measurements have been carried out on nanocrystalline thin films of CeO_2 or Gd^{3+}-doped CeO_2 deposited by screen printing on sapphire substrates: interesting correlations between microstructure and electrical conductivity have been described [15].

Presented at the OSSEP Workshop "Ionic and Mixed Conductors: Methods and Processes", Aveiro, Portugal, 10–12 April 2003

E. Gourba · A. Ringuedé (✉) · M. Cassir
Laboratoire d'Electrochimie et de Chimie Analytique—UMR 7575, CNRS-ENSCP, 11 rue Pierre et Marie Curie, cedex 05, 75231 Paris, France
E-mail: Armelle-Ringuede@enscp.jussieu.fr

P. Briois · A. Billard
Laboratoire de Science et Génie des Surfaces—UMR 7570, Ecole des Mines, Parc de Saurupt, 54042 Nancy, France

In this work, d.c. reactive magnetron sputtering of metallic Ce–Gd targets was used to deposit GDC thin layers, less than 5 μm thick, on stainless steel substrates which were systematically analysed by impedance spectroscopy in order to correlate the electrical properties with the thickness and microstructure.

Experimental

D.c. reactive sputtering

GDC thin films of thickness varying between 0.5 and 5 μm were sputter-deposited on glass slides and thin ferritic stainless steel substrates at low pressure (0.5 Pa) and low temperature (< 200 °C) by direct current sputtering of a metallic cerium–gadolinium (10 at.% Gd) target, 50 mm in diameter, in argon–oxygen reactive mixtures of various compositions. The experimental device is a 40-L sputtering chamber pumped down via a turbo-molecular pump, allowing a base vacuum of about 10^{-4} Pa. The sputtering conditions adopted in this study are stable because of a relatively high pumping speed compared with the area of the receptive surfaces. Hence, the oxygen partial pressure–oxygen flow rate curve is reversible with no hysteresis phenomenon. Hence, inevitable target erosion becomes significant in our reactor after about 3–4 h of deposition. The substrates are positioned at about 45 mm from the target axis, at a draw distance of about 110 mm. The target is mounted on an unbalanced magnetron and is powered by a 3-kW SAIREM pulsed d.c. supply, equipped with a fast arc detector able to cut microarcs within 1–2 μs. In all the experiments, the discharge current is maintained at a constant value of 0.5 A and the pulse frequency at 33 kHz. The flow rates of argon and oxygen are controlled with MKS flowmeters and the total pressure is measured using an MKS Baratron gauge.

Physicochemical characterisations

Optical transmission interferometry (OTI) was performed, using a halogen lamp ($\lambda = 550$ nm) as light source, through the glass substrate located at 45 mm from the magnetron axis, with a normal incidence. The signal, sent via an optical fibre to an Acton spectrometer with a 1,200 groove.mm^{-1} grating and a photomultiplier tube (Hamamatsu R 636), was recorded to a computer. Optical indexes and thicknesses of the coatings were obtained by fitting the interferometric measurements with a simple Matlab simulation program, following a theory developed elsewhere [18]. The thicknesses of the films were also measured by the step method, with a Talysurf profilometer, allowing an accuracy of the measurements of about 40 nm.

The structural features of the coatings were assessed by grazing angle (4°) X-ray diffraction (XRD:$\lambda_{kCo} = 0.17889$ nm) using an Inel diffractometer, and morphological features by scanning electron microscopy (SEM: Phillips XL30S.FEG). Finally, the intrinsic stress of the coatings was estimated via measurements after deposition of the resulting curvature of a thin cantilever steel foil (150 μm thick) using the Stoney formula [19].

Electrical characterisation

Electrical measurements were carried out using a frequency-response analyser, PGStat30 Autolab Ecochemie BV. A two-electrode configuration was used to realise impedance spectroscopy measurements. The metallic substrate (stainless steel) constituted the first electrode and a spiral of platinum wire the second one. The platinum electrode geometric surface was 0.35 cm^2. In order to separate the electrical contribution of the thin layer from the electrode response, the a.c. signal amplitude was varied from 100 to 300 mV. The measurements were realised from 1 MHz to 1 Hz, using 11 points per frequency decade. All measurements were carried out under atmospheric pressure, as a function of temperature, from 200 to 440 °C.

The impedance diagrams were deconvoluted using the fitting software EQUIVCRT, commercialised by Boukamp [20]. The equivalent capacitance was calculated from the following formula:

$$C_{eq} = R^{\frac{(1-n)}{n}} Y_0^{\frac{1}{n}}$$

where Y_0 and $n$are the parameters related to the constant phase element.

The relaxation frequencies were calculated using this equation:

$$F^0 = \frac{1}{2\pi (RY_0)^{\frac{1}{n}}}$$

Due to the non-symmetrical two-electrode configuration, the analytical calculation of the conductivity from the measured resistance has not been possible. Thus, only resistances are discussed in the paper and not the conductivity. In terms of geometrical parameter, the thickness of the deposited layers varied, but the surface of the electrodes was kept constant.

Results and discussion

The standard deposition conditions were determined according to three simultaneous criteria:

- The first consists of minimising the intrinsic stress level in order to allow the deposition of relatively thick coatings of about 5 μm without spalling.
- The second is ascribed to the deposition of films presenting a rather good thickness homogeneity along a distance from the magnetron axis, especially to guarantee convenient OTI measurements.
- The last is ascribed to the deposition of dense coatings.

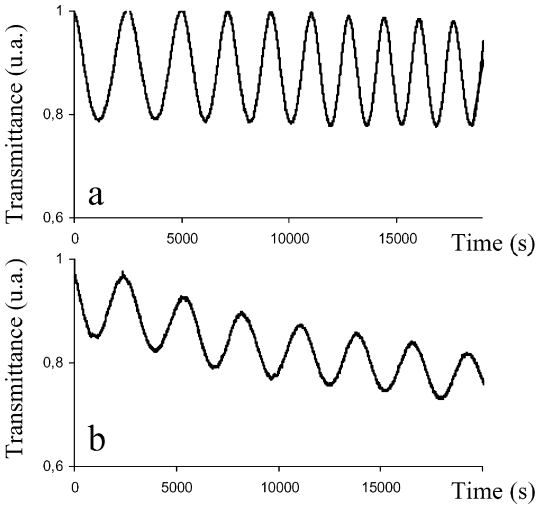

Fig. 1a,b OTI measurements vs. time performed in cases of a perfectly stoichiometric (**a**) and a substoichiometric (**b**) GDC film

Within the conditions adopted in this study, OTI measurements revealed the heating of the target. Indeed, in the case of insufficient oxygen flow rate introduced into the reactor, the coating, initially transparent, becomes more and more opaque during deposition, which leads to the deposition of a substoichiometric film as shown in Fig. 1b. It is thus necessary to increase the oxygen flow rate to guarantee the stoichiometry of the coatings, as seen in Fig. 1a. This behaviour is consistent with previous measurements performed as a function of the target temperature [21]. Indeed, as increasing the target temperature decreases its poisoning by oxygen, the higher the target temperature, the higher the deposition rate (i.e. frequency of the OTI signal) which can produce a loss in impinging oxygen at the surface of the substrate (i.e. attenuation of the OTI signal).

The GDC films deposited under the standard conditions crystallise in the expected suitable f.c.c. fluorine structure, as observed in Fig. 2. Obviously, the XRD spectra exhibit the substrate (110)α and (200)α lines only

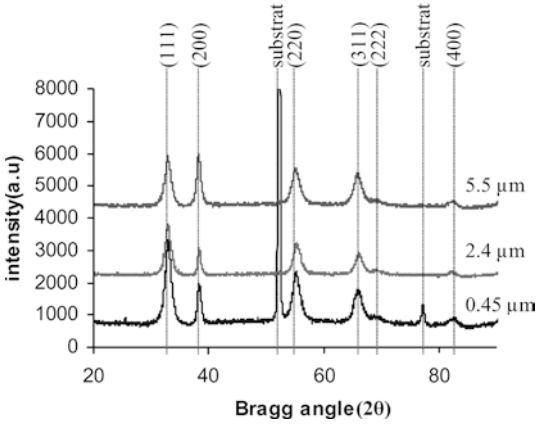

Fig. 2 XRD spectra performed with a 4° grazing incidence on GDC coatings of different thickness showing the convenient f.c.c. fluorine structure

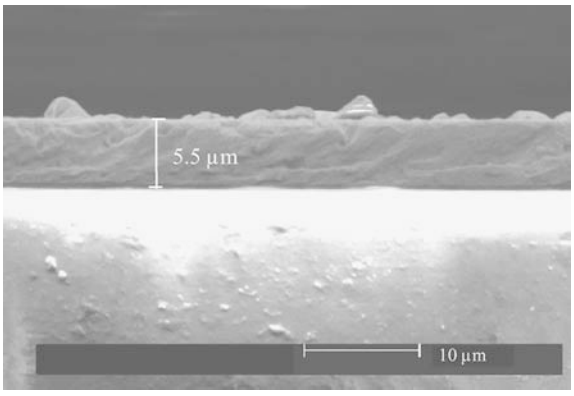

Fig. 3 SEM brittle-fracture cross section of a GDC coating, 5.5 µm thick, sputter deposited on a glass slide

for the thinnest films. The fact that change in neither the wideness of the peaks nor in their angular position is observed confirms that the film composition and microstructure are quite constant. As shown in the scanning electron micrograph in Fig. 3 performed on brittle-fracture cross sections, the coatings are dense and present low defect densities, which are expected to be favourable parameters to the ionic conductivity of O^{2-} whatever their thickness.

The electrical characteristics of three different layer thicknesses have been analysed. Considering a typical impedance plot, in Nyquist representation, two main contributions can be distinguished: the highest frequency contribution does not depend on the a.c. signal amplitude, in opposition to the lowest frequency contribution. An illustration is given in Fig. 4 at 320 °C in the case of the 5.5-μm GDC layer; the frequency limit was 10 kHz, as shown on both plots (Nyquist and Bode, Fig. 4 and Fig. 5, respectively). This allowed us to discriminate the layer response from the electrode response. Indeed, the GDC layer presents mainly ionic conduction under the temperature and oxygen partial pressure

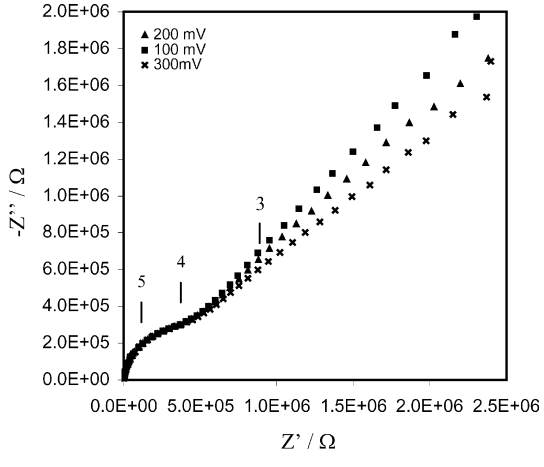

Fig. 4 Nyquist impedance plots of a 5.5-μm GDC layer, registered at 320 °C, as a function of a.c. signal amplitude. Logarithms of frequency are indicated in the figure. Only the frequency domain between 1 MHz and 100 Hz is reported

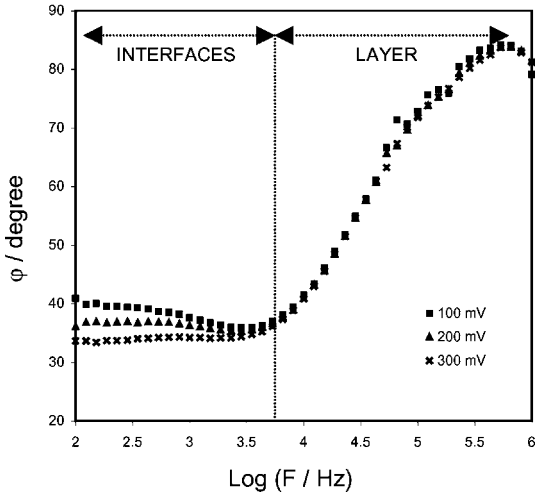

Fig. 5 Bode impedance plots of a 5.5-μm GDC layer, registered at 320 °C, as a function of a.c. signal amplitude

conditions used in this work. It is well known that it is easier to influence the electrode phenomena by signal amplitude than the electrolyte behaviour. Therefore, the well-defined semi-circle at high frequency corresponds to the layer contribution.

As mentioned in the experimental procedure part, only the thickness of the deposited layer varied. It allowed us to compare the different resistance but unfortunately without considering all the microstructure effects. So we have reported for the three layers the resistance and not the conductivity as a function of the temperature, in Arrhenius coordinates. These variations are reported in Fig. 6, in which the variation of the resistance follows an Arrhenius-type law with an associated activation energy of 0.94 eV. This value does not depend on the thickness, but is higher than the values of about 0.75 eV reported in the literature for sintered GDC samples [22, 23]. As expected, the layer resistance is lower when the thickness decreases. Srivastava et al. [24] observed an opposite tendency with thicker YSZ d.c. magnetron sputtered layers of more than 5 μm. In terms of impedance plots, compared to the sintered materials with two semi-circles (as a minimum), only one main semi-circle constitutes the layer response. This is commonly reported for nanoscaled materials, either for nanometre grain size or very thin layers [15]. Considering the relaxation frequency of a given contribution as a way to identify its origin (bulk or blocking effects, such as grain boundaries or porosity effects) [25], we have reported the calculated frequencies as a function of the temperature for each thin-layered sample and also for a 3.6-mm-thick sintered material (Fig. 7). As this parameter is not a function of the geometric factor related to the studied sample thickness and the electrode area, it can be justified to use it as a signature of each component of the electrical contribution. As shown by Schouler [25], considering one material composition, the bulk relaxation frequency is independent of the sample geometrical ratio. Thus, this parameter should be the same between sintered material and thin layers. Considering now the grain boundary (or blocking elements in general) relaxation frequency, the frequency range can be larger than for the bulk, due to the complexity of those elements (distribution in size, segregation effect...), but it is in the same order of magnitude. In the case of the studied layers, the observed high-frequency semi-circle seems to correspond to the blocking elements (grain boundaries, porosity...), and not to the bulk, as can be seen in Fig. 7, when superimposing relaxation frequencies for sintered samples and thin layers.

The activation energy associated with the variations of the relaxation frequency is the same as the energy associated with the layer resistance, confirming that the

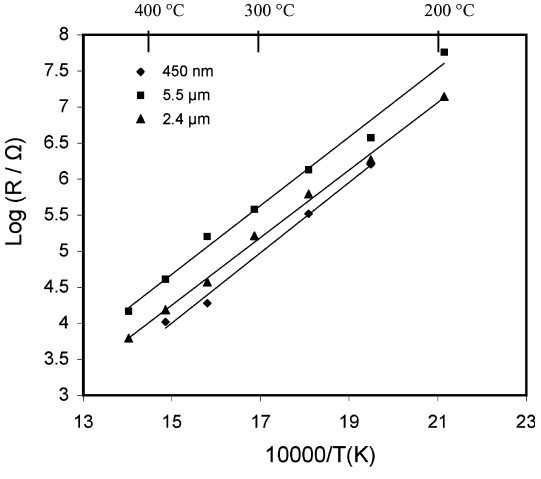

Fig. 6 Arrhenius plots of the layer resistance as a function of temperature, for three different thicknesses

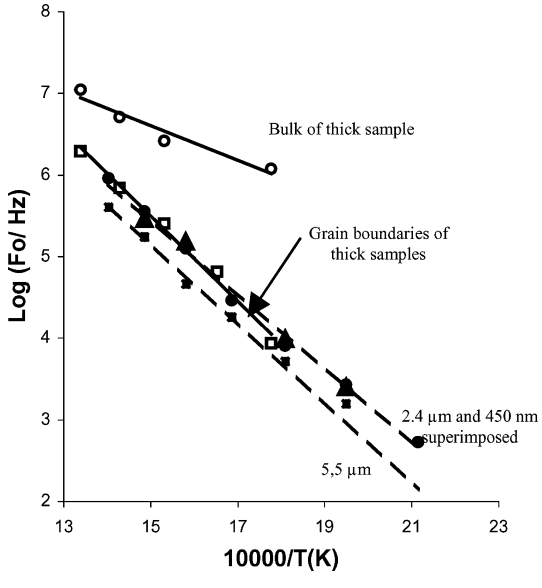

Fig. 7 Arrhenius plots of the relaxation frequency as a function of temperature, for the different thicknesses compared to the sintered sample

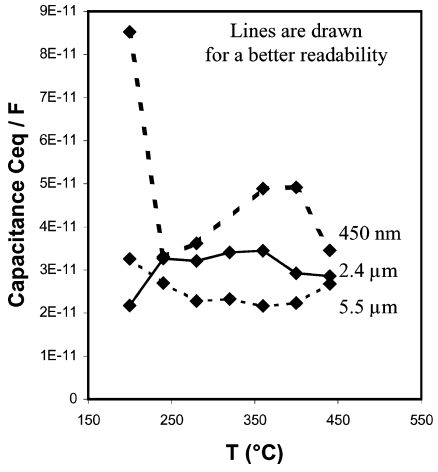

Fig. 8 Evolution of the equivalent capacitance as a function of temperature, for different thicknesses

equivalent capacitance remains constant with the temperature, as reported in Fig. 8 for each thickness.

Conclusions

Thin, dense and well-crystallised films of gadolinia-doped ceria have been deposited on stainless steel substrates by d.c. reactive magnetron sputtering. The electrical properties of the GDC thin layer were characterised by impedance spectroscopy, showing a preponderant contribution of the intergranular network compared to the bulk. This identification has been realised from the relaxation frequencies, and confirmed by the activation energy, which is higher for the grain boundary than for the bulk. The present study constitutes a preliminary work in order to evaluate the feasibility of GDC material as an SOFC electrolyte, whose operating temperature should be reduced. In the near future, GDC thin layer deposition will be carried out on the usual anode and cathode porous substrates, Ni–YSZ cermet and LSM. Nevertheless, according to literature data, determination of electrical features for thin layers prepared on porous substrates is more difficult than on dense and flat substrates, mainly because of the complexity of the electrode/electrolyte interface (adherence, active surface reaction, substrate porosity).

References

1. Perry Murray E, Tsai T, Barnett SA (1999) Nature 400:649
2. Park S, Vohs JM, Gorte RJ (2000) Nature 404:265
3. Hibino T, Hashimoto A, Inoue T, Tokuno JI, Yoshida SI, Sano M (2000) Science 288:2031
4. Riess I, Gödickemeier M, Gauckler LJ (1996) Solid State Ionics 90:91
5. Mori T, Yamamura H (1998) J Mater Synth Process 6:N3
6. Kim N, Kim NH, Lee D (2000) J Power Sources 90:139
7. De Souza S, Visco SJ, De Jonghe LC (1997) J Electrochem Soc 144:L35
8. Inoue T, Setoguchi T, Eguchi K, Arai H (1989) Solid State Ionics 35:285
9. Marques FMB, Navarro LM (1997) Solid State Ionics 98:191
10. Wang LS, Barnett SA (1992) J Electrochem Soc 139:2567
11. Srivastana PK, Quach T, Duan Y, Donelson R, Jiang SP, Ciacchi FT, Badwall SPS (1997) Solid State Ionics 99:311
12. Hayashi K, Yamamoto O, Nishigaki Y, Minoura H (1997) Solid State Ionics 98:49
13. Chan SH, Chen XJ, Khor KA (2003) Solid State Ionics 158:29
14. Lang M, Franco T, Schiller G, Wagner N (2002) J Appl Electrochem 32:871
15. Suzuki T, Kosacki I, Anderson HU (2002) Solid State Ionics 151:111
16. Peng R, Xia C, Liu X, Peng D, Meng G (2002) Solid State Ionics 152:561
17. Gourba E, Ringuedé A, Cassir M, Billard A, Päiväsaari J, Niinistö J, Putkonen M, Niinistö L (2003) Ionics 9:15
18. Perry F, Lelait L, Pigeat P, Billard A, Frantz C (1999) Vide Sci Tech Appl 291:285
19. Stoney G (1909) Proc R Soc Lond A 82:172
20. Boukamp BA (1986) Solid State Ionics 20:31
21. Billard A, Mercs D, Perry F, Frantz C (1999) Surf Coat Technol 116/119:721
22. Tianshu Z, Hing P, Huang H, Kilner J (2002) Solid State Ionics 148:567
23. Faber J, Geoffroy C, Roux A, Sylvestre A, Abélard P (1989) Appl Phys A 49:225
24. Srivastava PK, Quach T, Duan YY, Donelson R, Jiang SP, Ciacchi FT, Badwall SPS (1997) Solid State Ionics 99:311
25. Schouler E (1979) PhD thesis, Grenoble, France